Least dissipation cost as a design principle for robustness and function of cellular networks

Bo Han[1] and Jin Wang[1,2,*]

[1]*Department of Chemistry, Department of Physics, and Department of Applied Mathematics, State University of New York at Stony Brook, Stony Brook, New York 11794, USA*

[2]*State Key Laboratory of Electroanalytical Chemistry, Changchun Institute of Applied Chemistry, Chinese Academy of Sciences, Changchun, Jilin 130022, People's Republic of China*

(Received 5 February 2007; published 27 March 2008)

From a study of the budding yeast cell cycle, we found that the cellular network evolves to have the least cost for realizing its biological function. We quantify the cost in terms of the dissipation or heat loss characterized through the steady-state properties: the underlying landscape and the associated flux. We found that the dissipation cost is intimately related to the stability and robustness of the network. With the least dissipation cost, the network becomes most stable and robust under mutations and perturbations on the sharpness of the response from input to output as well as self-degradations. The least dissipation cost may provide a general design principle for the cellular network to survive from the evolution and realize the biological function.

DOI: 10.1103/PhysRevE.77.031922 PACS number(s): 87.15.−v

Understanding the function and stability of the cellular network requires a global characterization of the system. The nature of the network has been explored through various experimental techniques [1,2]. It is found that cellular networks are often quite stable and robust against intrinsic and environmental perturbations. There are an increasing number of bioinformatic studies on the global topological structures of the networks [3], as well as some studies from a physical perspective through underlying chemical reactions on the network robustness [2,4–7]. Recently, efforts have been made in understanding the biological function from an energy landscape perspective [8–15]. The advantage of this approach is that both global and local properties of the network can be explored in fluctuating environments [16,17]. In fact, explicit illustrations of the underlying energy landscape and robustness for MAP Kinase signal transduction, yeast cell cycle, and gene regulatory networks have been given recently [12–15].

These studies provided us insight into understanding the robustness of networks with a finite number of deep basins of attractions either through a funnel (one basin of attraction, for MAPK or yeast cell cycle) or multiple funnels (several basins of attractions for gene regulatory networks). The deep basins of attractions of the landscape might be the result of the evolution selection to perform the biological function and maintain the robustness. The question is then how the networks realize that. Cellular networks are open nonequilibrium systems due to interactions and exchanges with the environments. At steady state, both the steady-state probability or the corresponding landscape and the local flux are needed to characterize the nonequilibrium network. Contrary to the situation for the equilibrium case where the steady-state probability can characterize the whole system, the local flux is not necessarily zero in the nonequilibrium case because the detailed balance may not be satisfied. For an open nonequilibrium network, there are dissipation costs from the exchange with the environments which can be described using the underlying landscape and the flux for the system. Here we provide a possible evolution scenario: The network may have evolved to minimize the dissipation cost to realize the biological function, robustness, and structurally stability against genetic and environmental perturbations. Minimizing the dissipation cost might provide a design principle for evolution selection of biological functions and robust networks.

To explore the dissipation cost of a cellular network, we will use the budding yeast cell cycle as an example. We will summarize the previous robustness and landscape investigations [14] in Fig. 1 to serve as a basis for the current study. A network wiring diagram based on the crucial regulators was constructed [4,5] as shown in Fig. 1(a).

In Fig. 1(a), each protein node [5] is assumed to have only two states $S_i=1$ and $S_i=0$, representing the active and inactive states of the protein. There are 11 protein nodes in the network wiring diagram and all together 2^{11} states. Each state can be represented by S with a distinct combination of the on and off of the 11 protein nodes of Cln3, MBF, SBF, Cln1-2, Cdh1, Swi5, Cdc20, Clb5-6, Sic1, Clb1-2, and Mcm1 represented by $\{S_1,S_2,S_3,\ldots S_{11}\}=S$. $\rightarrow$ arrows represent positive regulations or activations (1). $\dashv$ arrows represent negative regulations or repressions (−1). The loop represents self-degradations to the nodes which are not regulated by others.

The significant intrinsic and extrinsic fluctuations within the cell imply that we should follow the probability evolution rather than deterministic dynamics in the network. The transition matrix T can be simplified by assuming the Markovian process [14,18]. The Markovian approximations is introduced here for simplicity. There can be time delays, for example, due to the presence of translation step in addition to transcription. This can be rendered by the introduction of more variables such as mRNA. Therefore we introduce the transition matrix: $T_{\{S_1(t'),S_2(t'),\ldots,S_{11}(t')|S_1(t),S_2(t),\ldots,S_{11}(t)\}}=\Pi_{i=1}^{11}T_{\{S_i(t')|S_1(t),S_2(t),\ldots S_{11}(t)\}}$ where t is the current time and t' is the next moment. The input-output switching response function has a similar form often seen in neural science [19]. The form of the response function although similar to the neural science can actually approximate the nonlinear in-

*Corresponding author: jin.wang.1@stonybrook.edu

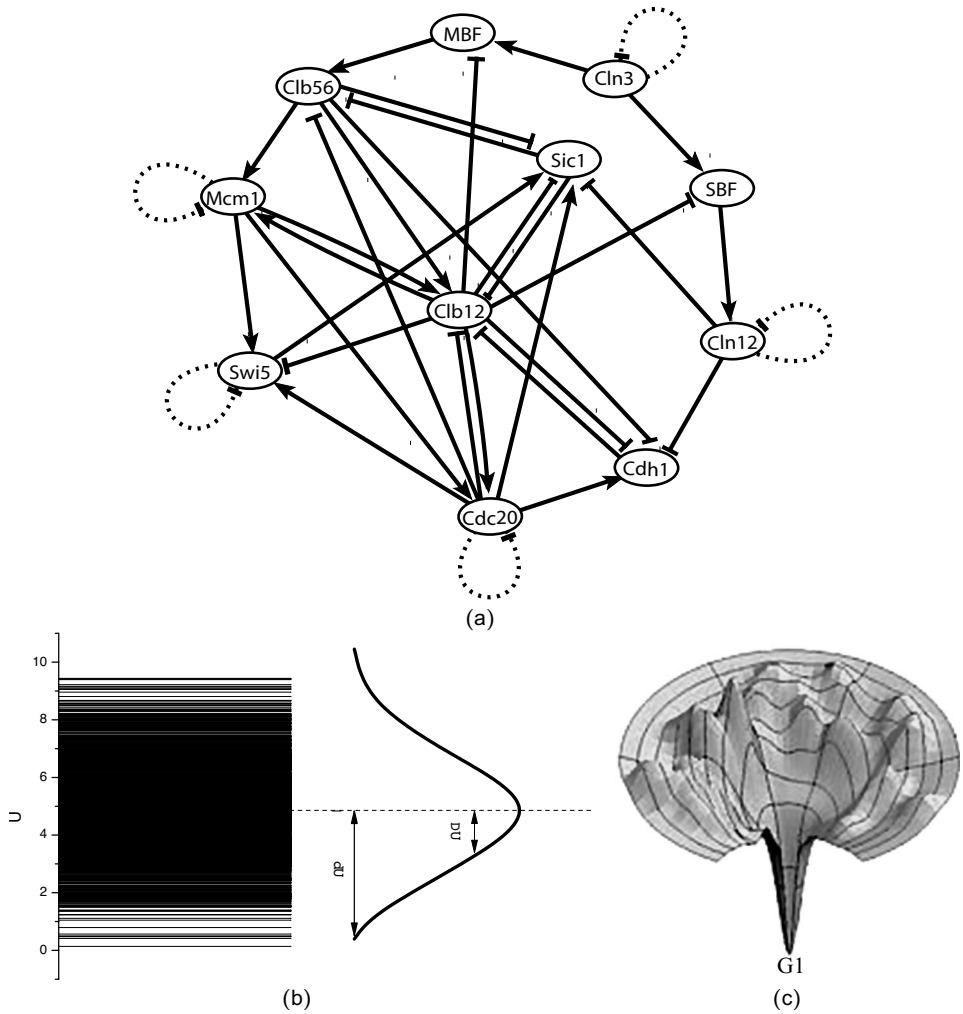

FIG. 1. (a) The yeast cell cycle network scheme: wiring diagram, → arrow represents positive activating regulations (1); ⊣ arrow represents negative suppressing regulations (−1); loop represents self-degradation. (b) The spectrum and the histogram or the distribution of the potential energy U. (c) An illustration of the funneled landscape of the yeast cell cycle network. The global minimum of the energy is at the $G1$ state.

crease of the protein number production upon regulations of others. It has been widely used in the literature [2,4]. The transition matrix can be defined as (with nonzero input): $T_{\{S_i(t')|S_1(t),S_2(t),\ldots S_{11}(t)\}}=\frac{1}{2}\pm\frac{1}{2}\tanh[\mu\Sigma_{j=1}^{11}a_{ij}S_j(t)]$. Furthermore, $T_{S_i(t')|S_1(t),S_2(t),\ldots S_{11}(t)}=1-c$ when there is no input of activation or repression $[\Sigma_{j=1}^{11}a_{ij}S_j(t)=0]$, c is a small number mimicking the effect of self-degradation. Here a_{ij} is the arrow or link representing the activating (+1) or suppressing (−1) interactions between the ith and jth protein nodes in the network, which is explicitly shown in the wiring diagram of Fig. 1. μ is a parameter controlling the sharpness or sensitivity of the response from input to output. $\frac{1}{\mu}$ can also be a measure of the fluctuation strength (for example, mimicking the effects of temperature) [14]. The fluctuation referred in this paper is a measure of the environmental noise or external noise, not directly the intrinsic noise from protein number fluctuations. When the environmental noise is low, then the response will be sharper.

With the transition probability among different states specified, we can write down the master equation for each of the 2^{11} states as $dP_i/dt=-\Sigma_j T_{ij}P_i+\Sigma_j T_{ji}P_j$ where T_{ij} (T_{ji}) represents the transition probability from state i (j) to state j (i) specified in details above. Here i and j are from 1 to $2^{11}=2048$ states and $\Sigma_{i=1}^{i=2^{11}}P_i=1$.

The steady-state probability distribution can be solved numerically [14]. One can link the steady-state probability distribution with the generalized potential energy as $U_i=-\ln P_i$ [9,10,12–15].

Figure 1(b) shows the spectrum as well as the histogram or distribution of U $(U=-\ln P_{\text{steady-state}})$. We can see that the distribution is approximately Gaussian. The global minimum of U was found to be the same state as the fixed point [the stationary $G1$ state=(0;0;0;0;1;0;0;0;1;0;0)] for the yeast cell cycle [14]. In quantifying the stability or robustness, we previously defined the robustness ratio (RR) [12–14] for the network as the ratio of the gap, δU, the difference between this global minimum of $G1$ state $U_{\text{global minimum}}$ and the average of U (mimicking the slope of the landscape), $\langle U\rangle$ versus the spread or the half width of the distribution of U (mimicking the roughness or trapping of the landscape), When the RR is significantly larger than 1, the global minimum ($G1$ state) is well separated and distinct from the average of the network potential spectrum. Since $P=\exp\{-U(x)\}$, the weight or population of the global minimum ($G1$ state) will be dominant. This leads to the global stability or robustness discriminating against others. It shows a funnel picture of energy going downhill toward the $G1$ state in the evolution of network states, as illustrated in Fig. 1(c). So the RR gives a quantitative measure of the shape or topography of the underlying landscape.

The network is an open system in nonequilibrium state.

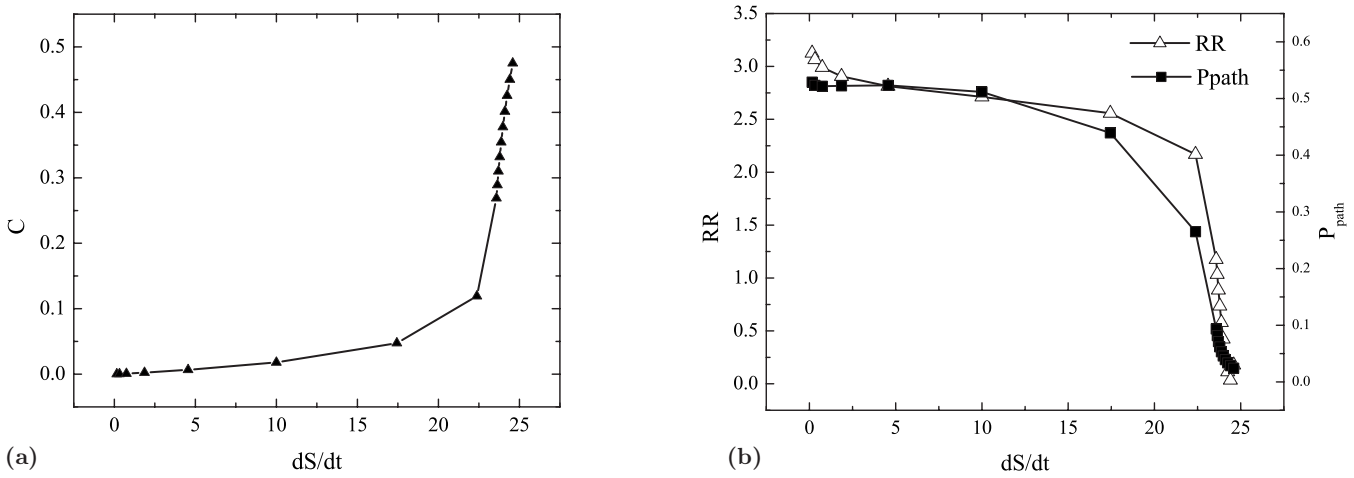

FIG. 2. Robustness and stability versus dissipation cost of the yeast cell cycle network for various protein self-degradation rate. (a) Self-degradation rate versus entropy production rate $\frac{dS}{dt}$. (b) Robustness ratio (RR) and probability of the biological path toward the $G1$ phase versus entropy production $\frac{dS}{dt}$ for various protein self-degradation rates.

Although we can obtain the steady-state probability and can define an equilibriumlike quantity, the local flux from j to i ($F_{ji_{\text{steady-state}}} = -T_{ij}P_{i_{\text{steady-state}}} + T_{ji}P_{j_{\text{steady-state}}}$) is not necessarily equal to zero (no detailed balance). The flux defines a generalized force for the nonequilibrium state along with the associated generalized chemical potential (from j to i) $A_{ji} = \ln(\frac{T_{ji}P_j}{T_{ij}P_i})$ [20–22]. There is a mapping between the cellular networks and electric circuits. The flux F_{ij} corresponds to current I, and the chemical potential A_{ij} corresponds to voltage V. The nonequilibrium cell network dissipates energy just as the electric circuits. In the steady state, the heat loss rate is related to the entropy production rate. The entropy production or dissipation characterizes "time irreversibility" and provides a lower bound for the actual heat loss in the Boolean network [11,20–22]. The total entropy change is equal to the part from the system or source plus the part from the bath or sink (dissipation). Since in steady state the entropy change of the system is equal to zero, the total entropy change (source) is equal to the entropy change of the sink (dissipation). The total entropy change (source) $=\Sigma F_i j A_i j$ is the entropy production and the sink term is dissipation. Therefore in steady state, knowing the entropy production, we know the dissipation quantitatively. The entropy S from the system part is defined as $S = -\Sigma_i P_i \ln P_i$ and entropy production rate (per unit time) $\frac{dS_{tot}}{dt}$ (system plus bath) is given by $\frac{dS_{tot}}{dt} = \Sigma F_{ji}A_{ji} = \Sigma_{ij} T_{ji}P_j \ln(\frac{T_{ji}P_j}{T_{ij}P_i})$. The entropy production rate is a characterization of the global properties of the network.

Equipped with the quantification of landscape and flux from the previous work [14] as illustrated in Fig. 1, we are now ready to explore the global nature of the network and the interrelationships between the robustness and stability with the dissipation cost in terms of entropy production under genetic and external perturbations (under different responses μ, self-degradations C, and mutations).

Figure 2(a) shows the self-degradation versus entropy production rate $\frac{dS}{dt}$ (at $\mu=5$). In [14], we show a less degradation c gives more robust network with large RR. Here we see that less self-degradation leads to less dissipation costs and less dissipation cost $\frac{dS}{dt}$ leads to more robust network with large RR and larger stability of the biological path toward the $G1$ phase.

Figure 2(b) shows the RR of the underlying energy landscape as well as the steady-state probability of the biological path toward the $G1$ phase versus entropy production $\frac{dS}{dt}$ with different self-degradation parameters c (at $\mu=5$).

We observe in Fig. 2(b) a relatively sharp decrease of the robustness through the RR and path probability P_{path} upon changing the self-degradation rate c. We noticed from previous studies that both the RR and P_{path} drop with an increase of self-degradation c (Fig. 7 in [14]). So the landscape changes significantly with the self-degradation. The entropy production rate is the accumulated effects from the combination of both landscape and flux. Therefore the entropy production rate is in general a nonlinear function of the accumulated effects of landscape and flux. The sharper transition of entropy production rate with respect to the stability upon changing the self-degradation might be from the more sensitive dependence on the accumulated landscape and flux.

We identified the preferential global pathway toward the global minimum $G1$ by following the most probable trajectory in each step of the kinetic moves from the deterministic equations of the corresponding to the master equations toward $G1$. Therefore the global path is referring to the deterministic path without the perturbations and noise. We explored the sum of the probabilities passing through this path in various conditions. When the perturbation or noise is small, we expect this path to be similar to the actual path. When the perturbation or noise is larger, we expect the actual path starts to deviate from this path. We expect to see less partition of the probabilities on this path. Obtaining the actual most probable path under various conditions is an important and challenging issue. We plan to investigate that in a future study.

The protein can be either 1 or 0, representing active or inactive. The 11 proteins are arranged in a vector form to represent the state of the system as (Cln3; MBF; SBF;

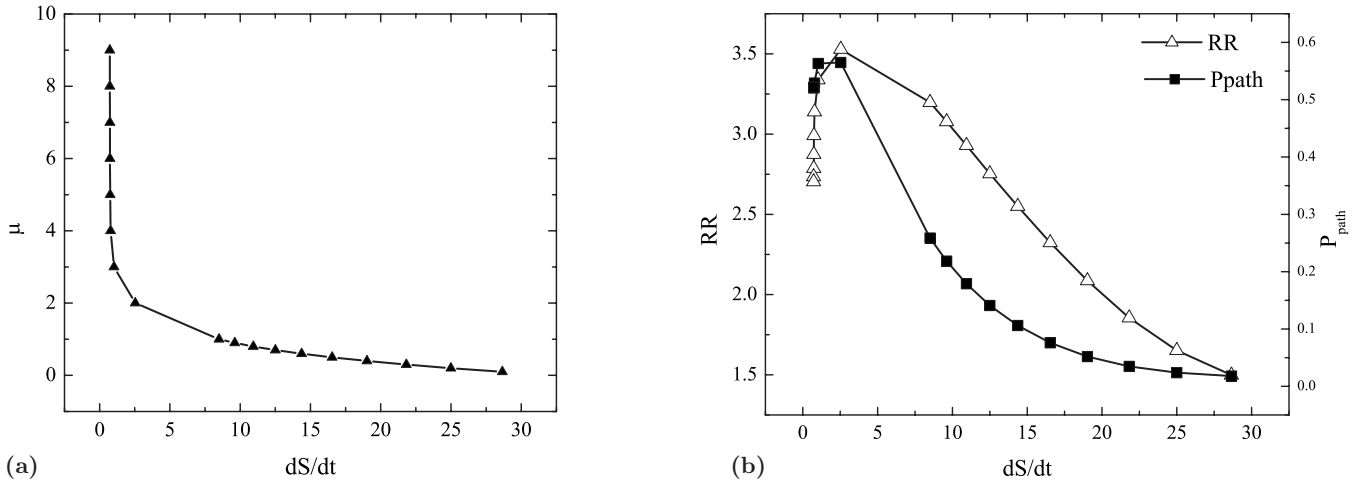

FIG. 3. Robustness and stability versus dissipation cost of the yeast cell cycle network for different responses or noise. (a) Response μ versus entropy production rate $\frac{dS}{dt}$. (b) Robustness ratio (RR) as well as steady-state probability of the biological path toward the $G1$ phase versus entropy production $\frac{dS}{dt}$ for different responses or noise.

Cln1,2; Cdh1; Swi5; Cdc20; Clb5,6; Sic1; Clb1,2; Mcm1). The most probable global path follows the states $1 \rightarrow 13$ sequentially toward $G1$ from the start signal where the start signal is in state sequence 1 given by (1;0;0;0;1;0;0;0;1;0;0). Three excited $G1$ states are in sequence 2, 3, 4, given, respectively, by (0;1;1;0;1;0;0;0;1;0;0), (0;1;1;1;1;0;0;0;1;0;0), (0;1;1;1;0;0;0;0;0;0;0). The S phase is in state with sequence 5 given by: (0;1;1;1;0;0;0;1;0;0;0). The $G2$ phase is in state with sequence 6 given by (0;1;1;1;0;0;0;1;0;1;1). The M phase is in states with sequence 7, 8, 9, 10, 11, given, respectively, by (0;0;0;1;0;0;1;1;0;1;1), (0;0;0;0;0;1;1;0;0;1;1), (0;0;0;0;0;1;1;0;1;1;1), (0;0;0;0;0;1;1;0;1;0;1), (0;0;0;0;1;1;1;0;1;0;0). The another excited $G1$ state is with sequence 12 given by (0;0;0;0;1;1;0;0;1;0;0). Finally, the stationary $G1$ phase is in state sequence 13 given by (0;0;0;0;1;0;0;0;1;0;0). The most probable path turns out to be the biological path going through $G1 \rightarrow S \rightarrow G2 \rightarrow M \rightarrow G1$ [14].

The rational of considering not only the $G1$ phase, but also the whole biological path of the cell cycle is as follows: As the cell cycle progresses, cells have to visit many different states on the biological path, not just stay in one state. The state of the $G1$ phase can be stable, but this may not imply that other states of the cell cycle are also stable. To create a robust cell cycle network all important states (local minimums on the potential) have to be investigated not just a stationary $G1$ phase (the global minimum). Therefore we include the probabilities of all the states on the biological path. In [14], we show a less degradation leads to more weight or stability for the $G1$ phase. Here we see that less self-degradation leads to less entropy cost and when entropy production $\frac{dS}{dt}$ decreases, the probability of the whole biological path including the stationary $G1$ phase also increases. This means that a less dissipation cost gives a more probable and stable biological path to the stationary $G1$ phase and therefore a more stable and robust network.

As mentioned before, robustness ratio here is a measure of the stability of the global minimum $G1$. If we consider the whole biological path, then the 13 local minimum states visited by the biological path should be grouped together. We expect a positive correlation between the stability of the global minimum $G1$ measured by the RR and that of 13 local minima constituting the whole biological path.

In Fig. 3(a), we plot the μ versus entropy production (per unit time) or the dissipation cost of the network, $\frac{dS}{dt}$. In [14], we show sharper response or less noise (larger μ) leads to more weight or stability for biological path including the $G1$ phase. Here we see that a sharper response and less noise lead to less entropy cost, and when the entropy production $\frac{dS}{dt}$ decreases, the probability of a biological path including the stationary $G1$ phase also increases.

In Fig. 3(b), we plot the robustness of the network and RR as well as the steady-state probability of the biological path toward the $G1$ phase versus entropy production (per unit time) or the dissipation cost of the network, $\frac{dS}{dt}$, for different μ (fixed $c=0.001$). In [14], we show that a sharper response or less noise (larger μ) in general leads to a more robust network with larger RR. We also show in that the presence of the peak of the RR is due to traps in the landscape [14]. On the right-hand side of the peak of the RR and steady-state probability of the biological path toward the $G1$ phase in Fig. 3(b), as the noise increases [μ decreases in Fig. 3(a)], the network quickly becomes unstable (smaller RR below 2.5 and probability of the biological path is below 0.3) and dissipation cost increases significantly. Here, we can see when the entropy production rate decreases, the RR and probability of the biological path toward $G1$ increase. The left-hand side of the peak of the RR and steady-state probability of the biological path toward $G1$ in Fig. 3(b) corresponds to a stable regime. The peak represents the most stable state. At the zero-noise limit, there are no fluctuations, so the system can easily get trapped in the local minimum of energy (local maximum of the steady-state probability). Increasing the noise level slightly from zero (larger μ) can help to adjust the system by overcoming the local traps to reach to the global minimum of energy [14]. Above all, we can see that a sharper response or less noise environments normally leads to less dissipation; the less dissipation cost gives a more

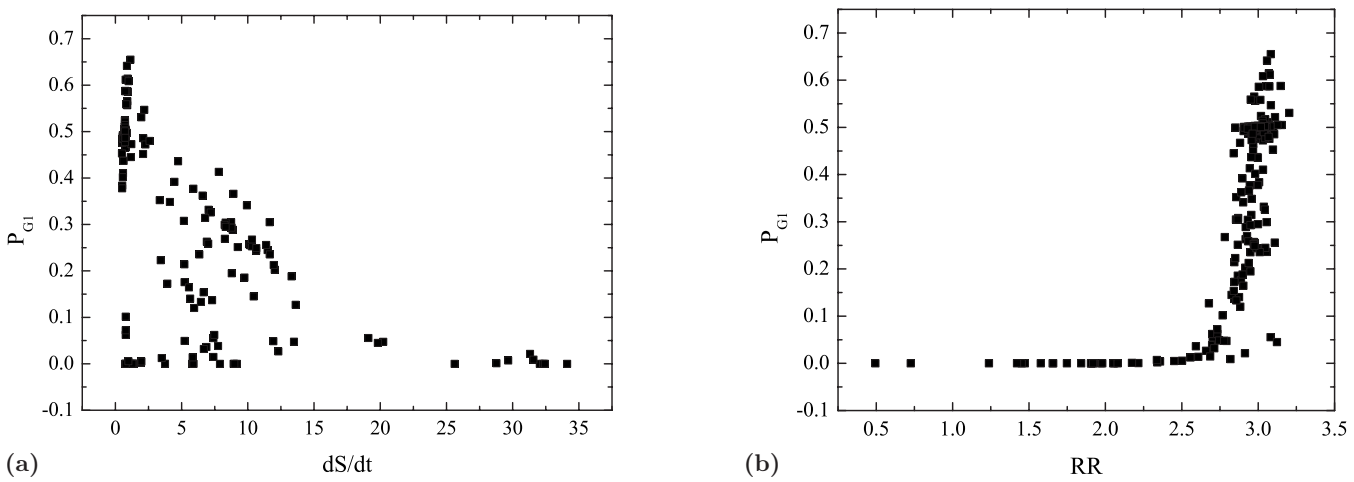

FIG. 4. Stability and robustness versus dissipation cost of the yeast cell cycle network for different perturbations through mutations. (a) Steady-state probability of $G1$, P_{G1}, versus entropy production rate $\frac{dS}{dt}$ for different mutations. (b) Robustness ratio (RR) versus steady-state probability of $G1$, P_{G1}, for different mutations.

probable and stable biological path and stationary $G1$ phase and therefore a more stable and robust network in general.

We also observe in Fig. 3(b) a relatively smooth decrease of the robustness through the RR (from high values to be below 2) and path probability P_{path} (from high values to below 0.2) upon changing the response μ (from high values to be below 1). We noticed from previous studies that both the RR and P_{path} drop sharply with the decrease of response μ (Fig. 6 in [14]). So the landscape changes significantly with the response. As mentioned above, the entropy production rate is the accumulated effects from the combination of both landscape and flux. So the entropy production rate is in general a nonlinear function of the accumulated effects of landscape and flux. The smoother transition of entropy production rate with respect to the stability upon changing the response might be from the less sensitive dependence on the accumulated landscape and flux.

Figure 4(a) shows the steady-state probability of the $G1$ (with $\mu=5$ and $c=0.001$) versus dissipation cost of the network against various mutations or perturbations through deleting an interaction arrow, adding an activating or repressing arrow between the nodes that are not yet connected in the network wiring diagram in Fig. 1, or switching an activating arrow to a repressing arrow or vice versa and deleting an individual node. Upon mutations, when the entropy production is smaller (larger), the $G1$ state tends to be more (less) stable and dominating. This is the regime where the underlying energy landscape is a funnel. We noticed that there are steady states with low entropy and low probability. Those are the outliers. They correspond to perturbed underlying energy landscapes which are either not very stable and unable to perform biological functions or possibly become significantly perturbed cell cycles (i.e., cycles without a stable $G1$ phase as in wild-type fission yeast cells). This implies that the dissipation cost and stability of the network through the $G1$ state might be more correlated in a relatively high-stability region while less correlated in a low-stability region. In other words, since the low-stability region often corresponds to a more fluctuating region, the dissipation cost is a less reliable measure of the network property. Therefore in this outlier regime, we may need to use both dimensions to explore the network, one for stability and one for function through dissipation cost.

Figure 4(b) shows the P_{G1} versus robustness ratio under various mutations mentioned above. We see that a larger (smaller) RR corresponds to a larger (smaller) P_{G1}. Since less entropy production leads to a more stable network (larger steady-state probability of $G1$, P_{G1}), therefore less entropy dissipation also leads to a larger RR and therefore more robust network. Random networks typically have a smaller RR and a smaller probability of $G1$ compared with biological ones, corresponding to rough underlying energy landscape. They are less stable and robust. The biological functioning network is quite different from the random ones in terms of the underlying energy landscape and stability. In the low-RR region, the robustness and entropy dissipation is less correlated. These networks are less of biological relevance.

Exploration of the relationship among statistical fluctuations, stability, robustness, and dissipation cost of networks here can be important for network design. The nature might evolves such that the network is robust against internal (intrinsic) and environmental perturbations and perform specific biological functions with minimum dissipation cost. From an evolution point of view, the fact that robustness and stability are often correlated with the entropy production rate may reflect the fact that more cost saving requires the system to have less fluctuations and perturbations, leading to a more robust and stable network. This may provide us a design principle of optimizing the connections of the network with minimum dissipation cost. In our study here this is also the equivalent of optimizing the robustness or stability of the network. The less dissipation cost or robust landscape therefore might be a quantitative realization of the Darwinian principle of natural selection at the cellular network level. The nature might evolve such that the biological networks become robust against perturbations and perform specific biological functions with minimum dissipation cost. The dis-

sipation criterion was also used in the context of constrained-based modeling of metabolic network [23].

Probing a nonequilibrium network is crucial for uncovering the mechanisms. We believe the dissipation cost is a quantitative measure of the nonequilibrium property which can be used to effectively show the noise level of the inherent system as seen in Fig. 3(a).

It is worthwhile to mention that there is a difference between cellular networks and the protein folding and binding problem [8,9]. In protein folding and binding, it is typically assumed that the quasiequilibrium condition and system obey the usual detailed balance conditions [8,9]. Therefore one can define the usual energy and potential. On the contrary, cellular networks are in a nonequilibrium state. There is no apparent energy or potential to use. We pointed out that we could still define the landscape as the $-\ln P_{\text{steady-state}}$, but we also need to take into account of the flux in addition to characterizing the whole nonequilibrium network. The entropy production rate which combines both the information of steady-state probability P and local flux can be used to globally quantify the nonequilibrium networks. An interesting and challenging question is to study the dissipation along the biological path. We will address this in a separate study.

J.W. would like to thank the NSF, ACS-PRF, and NSFC for financial support.

[1] E. H. Davidson *et al.*, Science **295**, 1669 (2002).
[2] C. Y. Huang and J. E. Ferrell, Jr., Proc. Natl. Acad. Sci. U.S.A. **93**, 10078 (1996).
[3] H. Jeong *et al.*, Nature (London) **407**, 651 (2000); S. Maslov and K. Sneppen, Science **296**, 910 (2002); R. Milo *et al.*, *ibid.* **298**, 824 (2002).
[4] J. J. Tyson, K. Chen, and B. Novak, Nat. Rev. Mol. Cell Biol. **2**, 908 (2001); K. C. Chen *et al.*, Mol. Biol. Cell **15**, 3841 (2004).
[5] F. Li *et al.*, Proc. Natl. Acad. Sci. U.S.A. **101**, 4781 (2004).
[6] J. E. M. Hornos, D. Schultz, G. C. P. Innocentini, J. Wang, A. M. Walczak, J. N. Onuchic, and P. G. Wolynes, Phys. Rev. E **72**, 051907 (2005).
[7] K. Kim, D. Lepzelter, and J. Wang, J. Chem. Phys. **126**, 034702 (2007).
[8] P. G. Wolynes, J. N. Onuchic, and D. Thrumalai, Science **267**, 1619 (1995); K. A. Dill and H. S. Chan, Nat. Struct. Biol. **4**, 10 (1997); M. Sasai and P. G. Wolynes, Proc. Natl. Acad. Sci. U.S.A. **100**, 2374 (2003).
[9] J. Wang and G. M. Verkhivker, Phys. Rev. Lett. **90**, 188101 (2003).
[10] X. M. Zhu *et al.*, Funct. Integr. Genomics **4**, 188 (2004).
[11] H. Qian and T. C. Reluga, Phys. Rev. Lett. **94**, 028101 (2005).
[12] J. Wang, B. Huang, X. F. Xia, and Z. R. Sun, Biophys. J. **91**, L54 (2006).
[13] J. Wang, B. Huang, X. F. Xia, and Z. R. Sun, PLOS Comput. Biol. **2**, e147 (2006).
[14] B. Han and J. Wang, Biophys. J. **92**, 3755 (2007).
[15] K. Kim and J. Wang, PLOS Comput. Biol. **3**, e60 (2007).
[16] H. H. McAdams and A. Arkin, Proc. Natl. Acad. Sci. U.S.A. **94**, 814 (1997).
[17] M. B. Elowitz and S. Leibler, Nature (London) **403**, 335 (2000); P. S. Swain, M. B. Elowitz, and E. D. Siggia, Proc. Natl. Acad. Sci. U.S.A. **99**, 12795 (2002); M. Thattai and A. van Oudenaarden, *ibid.* **98**, 8614 (2001).
[18] Y. Zhang *et al.*, Physica D **219**, 35 (2006).
[19] J. J. Hopfield, Proc. Natl. Acad. Sci. U.S.A. **79**, 2554 (1982).
[20] S. R. de Groot and P. Mazur, *Non-Equilibrium Thermodynamics* (Dover, New York, 1984).
[21] J. Schnakenberg, Rev. Mod. Phys. **48**, 571 (1976).
[22] H. Qian, Phys. Rev. E **65**, 016102 (2001).
[23] W. J. Heuett and H. Qian, J. Bioinf. Comput. Biol. **4**, 1227 (2006).